CANCER GENOMICS & PROTEOMICS *18*: 425-439 (2021)
doi:10.21873/cgp.20269

Biological Effect of Silver-modified Nanostructured Titanium Dioxide in Cancer

NEFELI LAGOPATI[1,2,3*], ATHANASSIOS KOTSINAS[1*], DIMITRIS VEROUTIS[1,3], KONSTANTINOS EVANGELOU[1], ANGELOS PAPASPYROPOULOS[1,3], MICHALIS ARFANIS[4], POLYCARPOS FALARAS[4], PARASKEVI V. KITSIOU[5], IOANNIS PATERAS[1], ANNA BERGONZINI[6], TERESA FRISAN[6], SPYRIDON KYRIAZIS[1], DIMITRIOS S. TSOUKLERIS[2,7], EFFIE-PHOTINI C. TSILIBARY[8], MARIA GAZOULI[9], EVANGELIA A. PAVLATOU[2] and VASSILIS G. GORGOULIS[1,3,10,11]

[1]*Laboratory of Histology-Embryology, Molecular Carcinogenesis Group, Medical School, National and Kapodistrian University of Athens, Athens, Greece;*
[2]*Laboratory of General Chemistry, School of Chemical Engineering, National Technical University of Athens, Zografou Campus, Athens, Greece;*
[3]*Biomedical Research Foundation Academy of Athens, Athens, Greece;*
[4]*Institute of Nanoscience and Nanotechnology, Laboratory of Nanotechnology Processes for Solar Energy Conversion and Environmental Protection, National Centre for Scientific Research "Demokritos", Athens, Greece;*
[5]*Institute of Biosciences and Applications, Laboratory of Biochemistry/Cell & Matrix Pathobiology, National Centre for Scientific Research "Demokritos", Athens, Greece;*
[6]*Umeå Centre for Microbial Research (UCMR), Department of Molecular Biology, Umeå University, Umeå, Sweden;*
[7]*NanoViis Company, Athens, Greece;*
[8]*Department of Neuroscience, University of Minnesota, Minneapolis, MN, U.S.A.;*
[9]*Department of Basic Medical Sciences, Laboratory of Biology, Faculty of Medicine, School of Health Science, National and Kapodistrian University of Athens, Athens, Greece;*
[10]*Faculty of Biology, Medicine and Health Manchester Cancer Research Centre, Manchester Academic Health Sciences Centre, University of Manchester, Manchester, U.K.;*
[11]*Center for New Biotechnologies and Precision Medicine, Medical School, National and Kapodistrian University of Athens, Athens, Greece*

Abstract. *Background/Aim: Nanomedicine is a promising scientific field that exploits the unique properties of innovative nanomaterials, providing alternative solutions in diagnostics, prevention and therapeutics. Titanium dioxide nanoparticles (TiO_2 NPs) have a great spectrum of photocatalytic antibacterial and anticancer applications. The chemical modification of TiO_2 optimizes its bioactive performance. The aim of this study was the development of silver modified NPs (Ag/TiO_2 NPs) with anticancer potential. Materials and Methods: Ag/TiO_2 NPs were prepared through the sol-gel method, were fully characterized and were tested on cultured breast cancer epithelial cells (MCF-7 and MDA-MB-231). The MTT colorimetric assay was used to estimate cellular viability. Western blot analysis of protein expression along with a DNA-laddering assay were employed for apoptosis detection. Results and Conclusion: We show that photo-activated Ag/TiO_2 NPs exhibited significant cytotoxicity on the highly malignant MDA-MB-231 cancer cells, inducing apoptosis, while MCF-7 cells that are characterized by low invasive properties were unaffected under the same conditions.*

*These Authors contributed equally to this work.

Correspondence to: Prof. Vassilis G. Gorgoulis, Laboratory of Histology-Embryology, Molecular Carcinogenesis Group, Medical School, National and Kapodistrian University of Athens, 75 Mikras Asias Str., Goudi, GR 11527, Athens, Greece. Tel: +30 2107462352, e-mail: vgorg@med.uoa.gr; Prof. Evangelia A. Pavlatou, Laboratory of General Chemistry, School of Chemical Engineering, National Technical University of Athens, 9 Iroon Politechniou Str., GR 15780, Zografou Campus, Athens, Greece. Tel: +30 2107723110, e-mail: pavlatou@chemeng.ntua.gr

Key Words: Nanomedicine, nanostructured titanium dioxide, silver-modified titanium dioxide, photocatalysis, cytotoxicity, apoptosis, anticancer properties.

Nanomedicine is an emerging inter-disciplinary scientific field that exploits the unique properties of innovative

nanomaterials, providing alternative solutions in diagnostics, prevention and therapeutics (1). In this framework, nanostructured titanium dioxide (TiO_2) has been thoroughly studied. The physical and chemical stability of TiO_2, high semi-conducting catalytic activity, interesting optoelectronic properties, low cost (2), high oxidative activity and relative ease of production are the main characteristics of this nanomaterial and for these reasons its potential has been exploited in various applications. Nowadays, since the pandemic emerged, a large number of masks and uniforms require sterilization more than ever before. Thus, photocatalysts, such as TiO_2 are promising candidates to provide protection even against SARS-CoV-2, offering bactericidal and virucidal activity. Due to the biocompatibility and the great spectrum of anticancer and antimicrobial properties, TiO_2 is utilized in various biomedical applications, such as in drug delivery systems (DDS), in molecular imaging as well as in alternative therapeutic approaches, in parallel with conventional methods or in replacement of them (3, 4).

TiO_2 can cause cytotoxicity (5) and induce apoptosis (6, 7). Various studies indicate that TiO_2 nanoparticles (NPs) can interfere through EGFR signaling pathways (8), leading to the inhibition of cell proliferation and survival, inducing senescence or apoptosis. During the early stages of cancer, senescence can act as an additional anti-cancer barrier, by inhibiting the propagation of incipient cancer cells, as apoptosis does (9). Intriguingly, senescence is also characterized by tumor promoting properties through a related secretory activity termed senescence associated secretory phenotype (SASP) (9). In this context, innovative alternative theranostics based on nanomedicine might focus on targeting of senescent cells (10).

The uptake of TiO_2 NPs in the cells, perhaps, can be achieved through endocytosis and passive diffusion. Since TiO_2 NPs behave as photocatalysts, when they are excited by photon energy derived from ultraviolet light (UV-A), pairs of holes and electrons are generated, reacting with the available water and oxygen, yielding reactive oxygen species (ROS) (11). This phenomenon can take place when TiO_2 NPs enter the cell and since the produced free radicals might be potentially very harmful (12), TiO_2 NPs may prove efficient damaging agents against crucial biomolecules of cancer cells. If this event is triggered controllably, it can specifically target the cancer cells, sparing the healthy ones. Such a scenario may be considered as the basis for the design and development of alternative therapeutic approaches.

The photocatalytic properties can be improved by several strategies. Chemical modification, dye-sensitization and coupling are among the most common techniques that are used for intervening in the properties of synthesized materials. Each of these methods is characterized by specific advantages and disadvantages (13). Chemical modification with metals or non-metals governs the physical-chemical properties of TiO_2, optimizing its photocatalytic and bioactive performance (14). Silver is used as a dopant, since it has the ability to trap the photo-excited electrons from TiO_2, allowing to the holes remain active (15). Thus, surface modification with silver reduces the recombination between the short-lived photoelectrons of the conduction band and the positive holes of the semiconductor band. Furthermore, silver particles have the ability to facilitate the electron excitation, since they can generate a local electric field (16). This field can be reasonably enhanced by the plasmon resonance effect due to the presence of the silver particles. According to many studies, chemical modification with silver increases the Specific Surface Area (SSA) of the TiO_2, improving its photocatalytic activity (17). In fact, silver modification promotes the ROS generation (18) prolonging the bioactivity duration of the TiO_2 NPs.

The aim of this study was the development of silver-modified TiO_2 NPs (Ag/TiO_2 NPs) with anticancer potential upon photoexcitation. The cytotoxic effects of Ag/TiO_2 NPs were examined on two cancer cell lines, derived from breast epithelium: a) MDA-MB-231 (human breast adenocarcinoma, highly invasive) and b) Michigan Cancer Foundation (MCF)-7 (low metastatic potential). Consequently, the cytotoxicity mechanisms induced by Ag/TiO_2 NPs were investigated, showing that Ag/TiO_2 NPs led to significantly higher cytotoxicity a significant the malignant MDA-MB-231 cancer cells, inducing apoptosis upon irradiation with UV-A light, while MCF-7 cells were not considerably affected.

Materials and Methods

Preparation of Ag/TiO_2 NPs. Ag/TiO_2 NPs were prepared through the sol-gel technique. Titanium (IV) butoxide (20 ml) was added in acidified aquatic solution under vigorous stirring. Then 30 ml of 1-butanol were added, leading to the formation of a clear sol-gel. An amount of silver nitrate ($AgNO_3$, Sigma-Aldrich, Darmstadt, Germany) was dissolved into deionized water and a final $AgNO_3$ solution of 0.75% w/v was obtained. Stirring for 24 h at room temperature (RT) followed. The pre-synthesized suspension was transferred into a stainless-steel chamber (autoclave) lined with Teflon material and was treated at 100˚C for 12 h, *via* the hydrothermal process. The precipitates were allowed to dry at 400˚C for 6 h and were purified, resulting in the production of Ag/TiO_2 NPs (19). The whole procedure was implemented in the dark.

Characterization of Ag/TiO_2 NPs. The synthesized nanopowders were characterized with respect to powder size, morphology, zeta-potential and bandgap. For this reason, X-ray diffraction (XRD), micro-Raman Spectroscopy, Infrared Spectroscopy, UV-Vis Spectroscopy, field emission gun scanning electron microscope, X-ray photoelectron spectroscopy and dynamic light scattering were employed.

The crystal phase determination and the crystallite size estimation of the Ag/TiO_2 NPs were carried out through the XRD method. X-ray diffraction analysis was held at a Siemens D-5000 diffractometer, operating at 40 kV and 35 mA with a Cu-K_α

radiation λ of 1.54 Å. The measurements were held at a 2-theta angle, a range between 20˚ and 80˚ and a scanning rate 0.1˚/min. The surface topography of the Ag/TiO_2 NPs was studied by a field emission gun scanning electron microscope (FEG-SEM, FEI Quanta 200F, FEI Company, Hillsboro, OR, USA). Prior to FEG-SEM investigations, 1 mg of powder were placed at the carbon tape and evaporated by gold to ensure conductivity.

Raman spectroscopy was applied to clarify the complexity of the structure of the produced Ag/TiO_2 NPs. The Raman device used was the inVia model from Renishaw (inVia, Renishaw, Wotton-under-Edge, Gloucestershire, UK). For measurement needs, a high power near infrared (NIR) diode laser (λ=785 nm) and a solid-state laser (λ=532 nm) were used as excitation sources, at RT in backscattering configuration. To avoid local heating and phase transformation, a ×100 short distance magnification lens, of low excitation power guided the laser beam, focusing onto the samples. The calibration of the frequency shifts was achieved through an internal Si reference. 3-4 spots were taken for each sample, with an exposure time of 30 s and 2-10 accumulations.

The surface chemical states of the Ag/TiO_2 NPs were analyzed by X-ray photoelectron spectroscopy (XPS-Particle size analyzer, Thermo K-Alpha). An ultra-high vacuum system (UHV), with base pressure 1×10^{-9} mbar, equipped with a monochromatic AlKα line at 1,486.6 eV was used for the photoemission experiments. A fitting routine was utilized for the XPS core level spectra analysis. This routine allowed the decomposition, of each spectrum into individual mixed Gaussian-Lorentzian peaks after a Shirley background subtraction. The powder-like samples had to be pressed in stainless steel pellets before the measurement. Survey spectra were acquired with a pass energy of 200 eV and a total of 10 scans with an energy step size of 1 eV. Valence band spectra were acquired using a pass energy of 50 eV and a total of 20 scans with an 0.1 eV energy step. High resolution scans of relevant elements were acquired with a pass energy of 50 eV and a total of 10 scans with an energy step size of 0.1 eV.

A UV-Vis spectrometer (U-3010, Hitachi, Tokyo, Japan) with an integrating sphere (50 mm) that allows diffuse reflectance measurements was used for the determination of the band gap (E_g) of the Ag/TiO_2 NPs. The light source was a deuterium lamp (DH2000), providing the light in the range of 210 nm – 1000 nm.

Finally, the size estimation and the zeta-potential of the Ag/TiO_2 NPs were determined *via* dynamic light scattering (DLS) by utilizing Zeta Sizer nano S (Malvern Inst., Malvern, UK). The average distribution of the NPs was estimated in aqueous dispersions, measured at different pH values (from 2 to 8) as it had been described previously in Lagopati *et al*. (6).

Cell culture. Two different cancer cell lines [MDA-MB-231 (human breast adenocarcinoma, highly invasive, ATCC - LGC Standards GmbH, Wesel, Germany) and Michigan Cancer Foundation MCF-7 (low metastatic potential, ATCC - LGC Standards GmbH)], both derived from breast epithelium, were used for the need of the experiments, focusing on the anticancer effect of Ag/TiO_2 NPs. The cells were cultured in 75 cm^2 flasks or petri dishes, in Dulbecco's modified Eagle's medium (DMEM) that was supplemented with 10% fetal bovine serum (FBS), 1% sodium pyruvate, 1% L-glutamine, and antibiotics (BioWest, Nuaillé, France); They were incubated at 37˚C in a 5% CO_2 incubator. Moreover, trypsin–EDTA: 0.05%/0.02% (w/v) (Gibco BRL, Life Technologies, Thermo Scientific, Paisley, UK) was utilized for the collection of cells (7).

Effect on cell proliferation. A cell population of about 100,000 cells/well was cultured in 6-well plates, in order to investigate the effect of the Ag/TiO_2 NPs on proliferation. Increasing concentrations of Ag/TiO_2 NPs dispersions were added to the appropriate plates, 24 h after plating. The samples were irradiated for 10 min, using four parallel UV-A light lamps (wavelength 350 nm, 3 mW cm^{-2}, Sylvania, OH, USA), into a lab-made photoreactor.

To avoid thermal effects, due to the possible temperature increase, a venting system was incorporated into the photoreactor and the samples were irradiated at a distance of 20 cm away from the lamps. The cells were allowed to rest for 24 h and were then stained with Trypan Blue and counted utilizing a hemocytometer (Neubauer, Corning, the Netherlands) and an Optical Microscope (OLYMPUS IM, Olympus Deutschland GmbH, Hamburg, Germany) (20). Measurements were taken until 96 h after illumination and the experimental procedure was repeated at least three times in triplicate.

Cell-viability analysis (MTT assay). 3-(4,5-dimethylthiazol-2-yl)-2,5-diphenyl-tetrazolium bromide (MTT) colorimetric assay Thiazolyl Blue Tetrazolium Bromide, M5655, Sigma-Aldrich, Darmstadt, Germany) was employed for the estimation of cell viability. Based on the functional principle of the MTT Assay and considering that the highest the number of viable cells, the highest the level of the formazan products, and consequently the highest the optical density value (21), the quantitation of cell viability, was achieved through the use of a multi-well scanning spectrophotometer (enzyme-linked immunosorbent assay reader). The optical density was measured at 570 nm and also at 650 nm, for normalization against the background (22).

For the experimental needs of the MTT assay, MCF-7 and MDA-MB-231 cells (~10.000 cells/well) were cultured in 96-well plates. Increasing concentrations of the Ag/TiO_2 NPs were added to the appropriate samples, 24 h after plating. Afterwards, the samples were irradiated using UV-A light for 10 min, and allowed to rest for 48 h.

According to the protocol that it has already described in a previous study of Lagopati *et al*. (7), the optical density was measured and the percentage of viability was estimated compared to untreated cells. The experiment was repeated five times in quadruplicate with similar results.

Western blotting. Western blotting experiments were performed to investigate the effect of the Ag/TiO_2 NPs on caspase-mediated poly(adenosine diphosphate ribose) polymerase (PARP) cleavage, as an indication of selective cell apoptosis. A protocol that was previously described in the study of Lagopati *et al*. (6) was employed for cell lysis and protein quantitation. Membranes were probed with anti-PARP (9542; Cell Signaling Technology, Bioline Scientific, Athens, Greece), anti-Bcl-2 (sc-7382), anti-Bcl-xL (sc-8392), anti-Bax (sc-7480), and anti-Bad (sc-9292) (Santa Cruz Biotechnology, Dallas, TX, USA) antibodies. An enhanced chemiluminescence detection system (Life Technologies, Thermo Scientific, Paisley, UK) was used for the protein detection, after incubation with horseradish peroxidase-conjugated secondary antibodies (GE Healthcare, Life Sciences, Amersham, Little Chalfont, Buckinghamshire, UK). The blots were stripped (Merck Millipore ReBlot Plus Kit and Reagents, Thermo Scientific) and reprobed with anti-β-tubulin (ab179511) monoclonal antibodies (Abcam, Cambridge, UK). Three independent experiments were implemented.

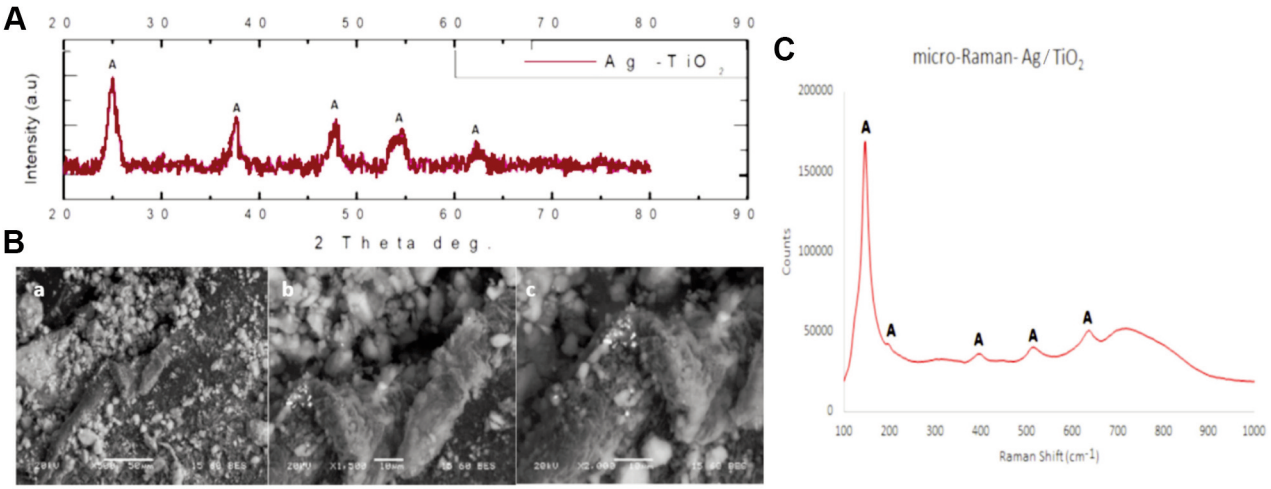

Figure 1. *(A) X-ray diffraction patterns (XRD) of Ag/TiO_2 NPs (silver-modified TiO_2 nanoparticles). Anatase (A) is the dominant crystal phase of Ag/TiO_2, with the highest intensity diffraction peak of anatase being at (2θ)=25.35˚ (2-theta angle), corresponding to (1 0 1) crystal plain. All the other detected peaks of A which are spotted are in accordance with the ICDD File No 03-065-5714. (B) FEG-SEM (Field emission gun scanning electron microscope) images of Ag/TiO_2 NPs at ×500 (a), ×1,500 (b) and ×2,000 magnification (c). (C) Raman spectrum of Ag/TiO_2 NPs. The spectrum identifies the formation of single anatase nano-crystalline phase, as all the peaks corresponding to the Raman fundamental modes of pure anatase crystal phase are located at 143 [Eg(1)], 197 [Eg(2)], 395 [B1g(1)], 514 (A1g), and 640 [Eg(3)] cm^{-1}.*

DNA-laddering assay. DNA was isolated from each sample and separated by agarose gel electrophoresis, according to the previously described protocol at Lagopati *et al*. (6). Images of intact and/or laddered DNA were obtained to certify the effect of the Ag/TiO_2 NPs on apoptotic cell death.

3D organotypic model development. Airway fibroblasts were embedded in type I collagen, allowing contraction of the gel mimicking the underlying submucosa. Positively selected HBEC-CDC6 Tet-ON (normal human bronchial epithelial) cells were seeded on top of the contracted layer and upon attachment of HBECs on the underlying stroma, the organotypic culture was submerged into the appropriate medium and then lifted to an air-liquid interface, while cell growth was performed at 37˚C with 5% CO_2. Matrigels were collected, formalin fixed, and paraffin embedded (23).

Statistical analysis. Values in each experiment are presented as means±standard deviation and statistically significant differences between the values of the samples were evaluated by one-way analysis of variance (ANOVA) as well as the nonparametric Kruskal–Wallis method using SPSS (IBM Corporation, Armonk, NY, USA); $p<0.05$ value was considered as statistically significant. We initially chose ANOVA since it allows the total variance to be broken down into 2 parts: the variation within each sample and the variation between the groups. Thus, it is the best choice for cross checking all treatment conditions (control, UV-A, Ag/TiO_2, photoexcited Ag/TiO_2, cis-platin) (24). However, we additionally utilized the nonparametric Kruskal–Wallis test (25), since the number of our measurements did not allow us to verify whether the values follow a normal distribution or not. The results that were obtained from the two methods were similar. Moreover, the Bonferroni method was employed as a posthoc tool to specify the pairs of analyzed data that are statistically significantly different (26).

Results

Ag/TiO_2 NPs Characterization. The crystallinity of the Ag/TiO_2 NPs was examined through XRD. Figure 1A depicts the recorded X-Ray diffraction diagram. Anatase (A) was the dominant crystal phase of TiO_2 that was detected, with the highest diffraction peak intensity being at 2θ=25.35˚, which corresponds to the anatase (101) crystal phase. The rest of the detected peaks of anatase that were spotted were found in accordance with the ICDD File No 03-065-5714. The average crystallite size of the TiO_2 powders can be estimated through Scherrer's equation (Equation 1):

$$d = \frac{0.89\lambda}{\beta \cos\theta} \quad (1)$$

where d goes for the average crystalline size, 0.89 corresponds to the Scherrer's constant, λ goes for the X-ray wavelength, θ is the diffraction angle and β stands for the FWHM (full-width-half-maximum). Using the main peak of anatase (101) at 2θ=25.35˚ (27), the average crystallite size of the Ag/doped TiO_2 NPs was estimated to be approximately 17 nm.

Ag/TiO_2 NPs morphology was examined by Field Emission Scanning Electron Microscopy (FEG-SEM). Selected images are shown in Figure 1B. It seems that the tested Ag/TiO_2 NPs consist of grains in the range of nanometers and there is homogeneity. These data are in agreement with the aforementioned XRD results.

Figure 1C presents the Raman spectrum of the Ag/TiO_2 NPs, identifying the formation of single anatase nano-

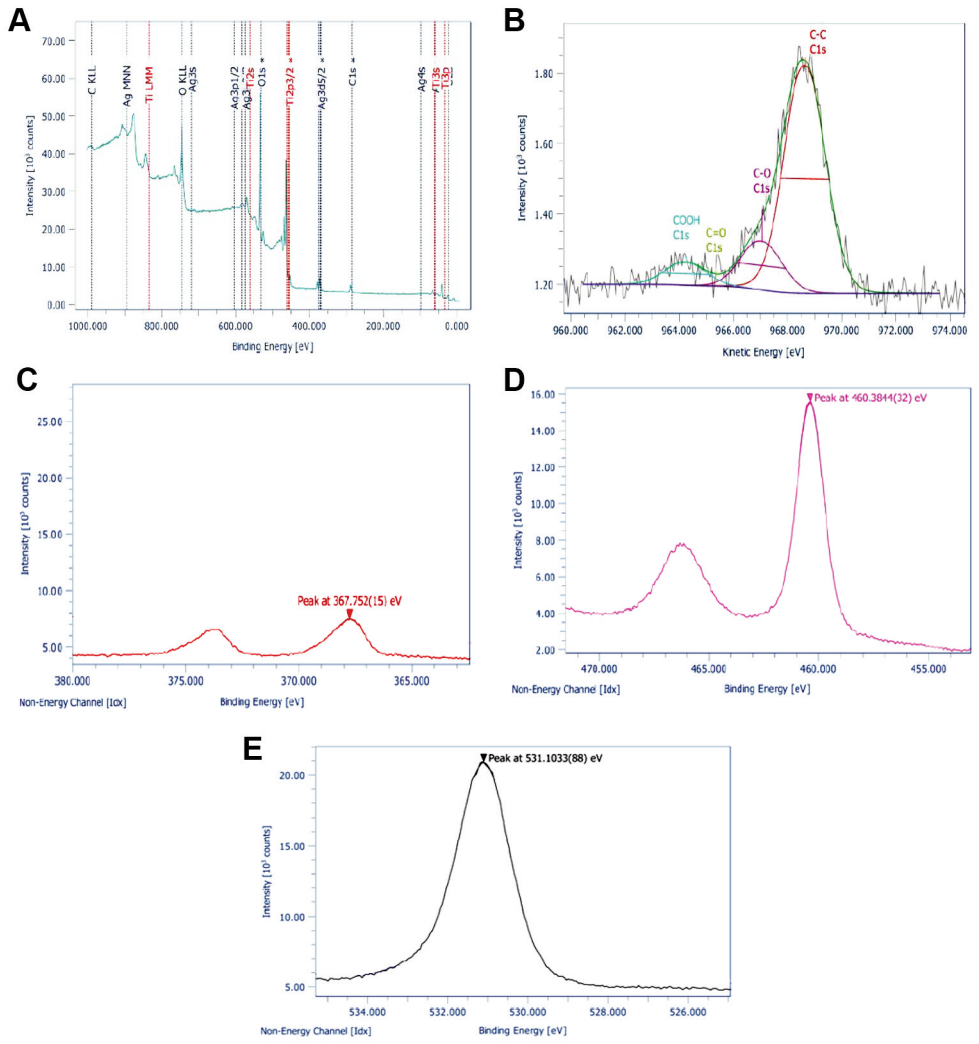

Figure 2. *(A) Wide survey with high resolution XPS (X-ray photoelectron spectroscopy) spectra of Ag/TiO_2 NPs (silver-modified TiO_2 nanoparticles) for (B) C1s, (C) Ag3d, (D) Ti2p and (E) O1s.*

crystalline phase. This finding was obtained through the observation of all the peaks which correspond to the Raman fundamental modes of pure anatase crystal phase, located at 143 [Eg(1)], 197 [Eg(2)], 395 [B1g(1)], 514 (A1g), and 640 [Eg(3)] cm−1. This result indicates the stabilization effect for the anatase phase as well as the inhibition of the anatase-brookite-rutile phase transformation, which was related to the silver treatment. These findings are in accordance with the relevant literature for Raman analysis (28).

XPS analysis was also performed in order to examine the elemental composition and the superficial chemistry of the Ag/TiO_2 NPs. All expected peaks according to the chemical synthesis protocol and design were detected. Thus, Ti2p (TiO_2 state), O1s (O in TiO_2 state), C1s (hydrocarbon state) were obtained through XPS analysis. Figure 2A depicts the wide survey spectrum of Ag/TiO_2 NPs, detecting the peaks of Ti, O, Ag and C. Figure 2B shows a detailed spectrum of C1s in high resolution, analyzed in C-C bonds in suboxides/hydroxides (C-O), carbonyl (C=O) and carboxyl groups (COOH). Carbonyls were not detected. X-Ray Induced Auger Electron Spectroscopy was employed for the identification of the silver. The modified Auger parameter was detected at 724.7 eVm due to the silver oxide. The FWHM of Ag3d is wide enough, due to the presence of silver oxide. Figures 2C, 2D, 2E show the detailed spectra of Ag3d, Ti2p and O1s, respectively, in high resolution. Table I presents the compositional analysis, after the correction process for the sensitivity factors and the characteristics of the transit analyzer.

UV-Vis spectroscopy allows the estimation of the Eg of the Ag/TiO_2 NPs. The presence of the metal dopant on the

Table I. *Compositional analysis of Ag/TiO_2 (silver-modified TiO_2).*

Name	Peak BE/eV	Compound	Atomic %
$Ti2_{p3/2}$	460.3	TiO_2	25.76±0.14
C1s	285.2	Hydrocarbon	16.61±0.22
O1s	531.1	O in TiO_2	56.15±0.3
$Ag3_{d5/2}$	367.7	AgO	1.48±0.01

surface of TiO_2 NPs leads to a wide absorption bands, which is a characteristic of localized surface plasmon resonance (LSPR) absorption phenomenon. This is common in cases of metal-structures like silver and silver coated TiO_2 NPs, according to literature (29). Visually, the Ag/TiO_2 NPs are quite grey and not totally white compared to pure TiO_2. This process of observed photochromism of the powders is associated with metal oxidation and reduction on the particles' surface. The position of the LSPR band center depends directly on the average particle size. Figure 3A presents the absorbance spectra converted to the Kubelka–Munk function, F(R), defined in equation 2 as (30):

$$F(R) = \frac{a}{S} = \frac{(1-R)^2}{2R} \quad (2)$$

where α is the molar absorption coefficient, S the scattering factor and R is the absolute reflectance. This methodology is usually utilized for samples, exhibiting high absorbance or light scattering (30).

The band gap energy (Eg) was calculated by using Tauc's equation (Equation 3):

$$(ahv) = A(hv - E_g)^n \quad (3)$$

where A is a constant and n=2 for indirect allowed transition (31).

In fact, by employing the Kubelka-Munk method extrapolating the linear portion of (F(R)*hv)1/2 vs. hv, the bandgap was estimated at 3.1 eV (Figure 3B), which is very close to the relevant Eg of the pure TiO_2 (3-3.2 eV). Thus, Ag/TiO_2 has the ability to be photo-excited upon irradiation with UV light.

Finally, DLS was employed for the determination of the hydrodynamic radius zeta potential of Ag/TiO_2. The pH was 6.7-6.8. The hydrodynamic radius distribution as a function of intensity and the zeta potential are shown in Figure 4 and B, respectively. It seems that the size distribution of the Ag/TiO_2 presents a maximum approximately at 145 nm, with a coefficient of variation (CV)~0,99%. The zeta potential was found as ZP=(–14.8±8) mV, with a CV~40%, meaning that the dispersion was prone to form agglomerates. Thus, rigorus mixing and the use of ultrasounds to break the aggregations were employed, shrinking the size of the NPs, and optimizing their stability before their administration to cell cultures.

Biological Effect of Ag/TiO_2 NPs

Effect on cell proliferation. In order to investigate the effect of Ag/TiO_2 NPs on cell proliferation, MCF-7 and MDA-MB-231 cells were cultured (~100,000 cells per well), with NPs dispersion concentration varying in the range of 0-0.8 mg/ml. The cell number was estimated and recorded as a function of time to generate growth rates. As a positive control for the experiments, cells treated for 24 h with cisplatin (0,8 mg/ml) were used. Cells treated with UV-A light without Ag/TiO_2 NPs were also utilized as an extra internal negative control, in order to ensure that the observed effect is not relevant to the irradiation itself. Therefore, we were able to exclude the case of the existence of thermal effects such as hyperthermia which would be a possible mechanism resulting in the inhibition of cell proliferation. It seems that there is no significant effect detected on cell proliferation for the MCF-7 cells, (Figure 5A). Upon irradiation with UV light there was also no significant effect on cell proliferation (Figure 5B). However, cell proliferation of the MDA-MB-231 cells, gradually inhibited in the presence of photoexcited Ag/TiO_2 NPs. A slight decrease was also observed in the presence of 0,8 mg/ml Ag/TiO_2 even without irradiation (Figure 5C). The highly malignant MDA-MB-231 cancer cells are proven o be more susceptible to the inhibition of cell proliferation or to cell death, exposed to photoexcited Ag/TiO_2 NPs (Figure 5D), compared to MCF-7 cells, which are not metastatic. Herein, a cell-dependent toxicity was observed (6, 7) and this cell behavior could be explained if we consider the different nature of the two cell lines. Moreover, the membrane receptors could be different and consequently, they interact with the NPs in a different way, leading to a different biological effect (32).

Cell-viability analysis (MTT assay). The MTT colorimetric assay was employed to estimate the cytotoxic effects of Ag/TiO_2 NPs on the viability of both cell lines. Hence, MDA-MB-231 and MCF-7 cells (~10,000 cells per well) were incubated, with increasing concentrations of the NPs for 48 h. The estimation of the percentage of cell viability as a function of the photocatalyst concentration was achieved through the Equation 4:

$$Cell\ Viability = \frac{OD_{treated\ sample} - OD_{background}}{OD_{untreated\ sample} - OD_{background}} \cdot 100\% \quad (4)$$

where O.D. is the Optical Density measured for each sample. A gradual decrease in cell viability was observed, as the concentration of Ag/TiO_2 NPs increased. More specifically, a concentration of 0,8 mg/ml Ag/TiO_2 reduced MDA-MB-231

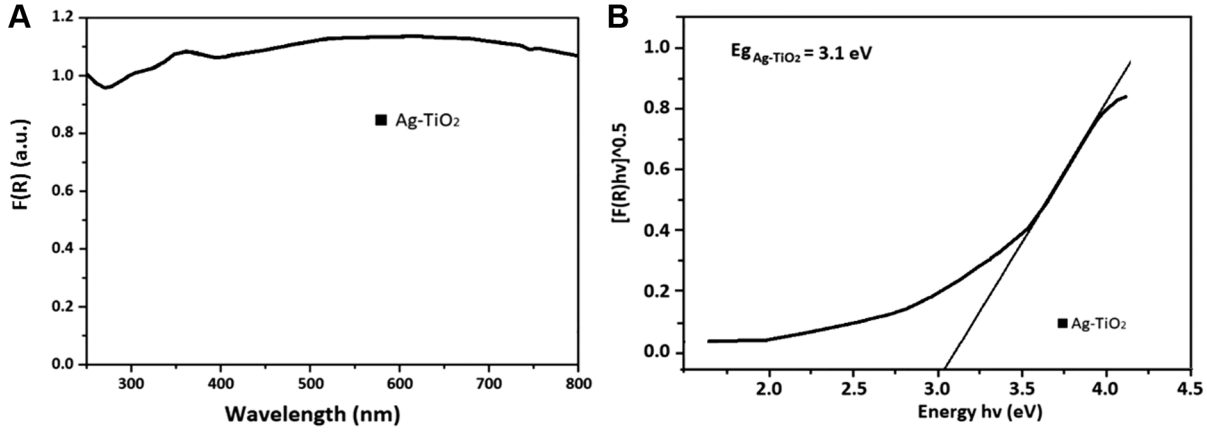

Figure 3. *(A) Variation of F(R) reflectance vs. wavelength for Ag/TiO_2 NPs (silver-modified TiO_2 nanoparticles) and (B) Optical band gap energy of Ag/TiO_2.*

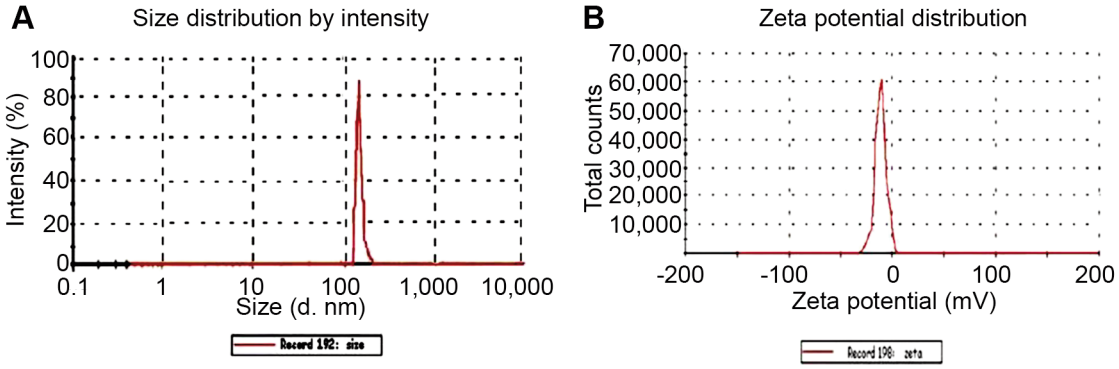

Figure 4. *Dynamic light scattering (DLS) results. Distribution of the (A) hydrodynamic diameter (d, or 2Rh) and (B) zeta potential of the Ag/TiO_2 NPs (silver-modified TiO_2 nanoparticles).*

cell viability by 20%, while the MCF-7 cells were not significantly affected (Figure 6A). The cytotoxic effect was more significant upon UV irradiation. Photo-activated Ag/TiO_2 reduced 40% the MDA-MB-231 cell population, while the same dose did not affect MCF-7 cells (Figure 6B). These series of experiments also showed a selective cytotoxicity of Ag/TiO_2. Possibly, the composition of the cell membrane proteins is different in each cell line and consequently the interactions between those proteins and Ag/TiO_2 NPs are different in each case. This hypothesis could explain why the MCF-7 cells were not affected at all. It is also well established that stem cell characteristics are demonstrated in the the triple negative MDA-MB-231 cells, like high expression of cancer stem cells (SCCs) markers $CD44^+/CD24^{low/-}$ and high activity of aldehyde dehydrogenase (ALDH). These features are associated with stem cell self-protection (33). The presence of the xenobiotic transporter (BCRP) on MCF-7 cells can also explain their resistance in this treatment, since BCRP is considered to contribute to multi-drug resistance (34).

Apoptosis activation upon Ag/TiO_2 or photo-activated Ag/TiO_2 treatment. It is well known that cell apoptosis is characterized by various morphological, biochemical and functional changes that are mediated by the activation of caspases. One of the main cleavage targets of activated caspases is PARP (113 kDa). PARP plays an important role in DNA repair, responding to an exposure to stress stimuli (35). PARP cleavage leads to an impaired enzymatic DNA-repair potential. In this regard, PARP cleavage can provide a reliable marker of cells that undergo programmed cell death (36, 37).

Western blot analysis was employed for the examination of PARP cleavage in both MCF-7 and MDA-MB-231 cells that treated with Ag/TiO_2 or photo-activated Ag/TiO_2. Furthermore, cell lysates from samples that had been treated

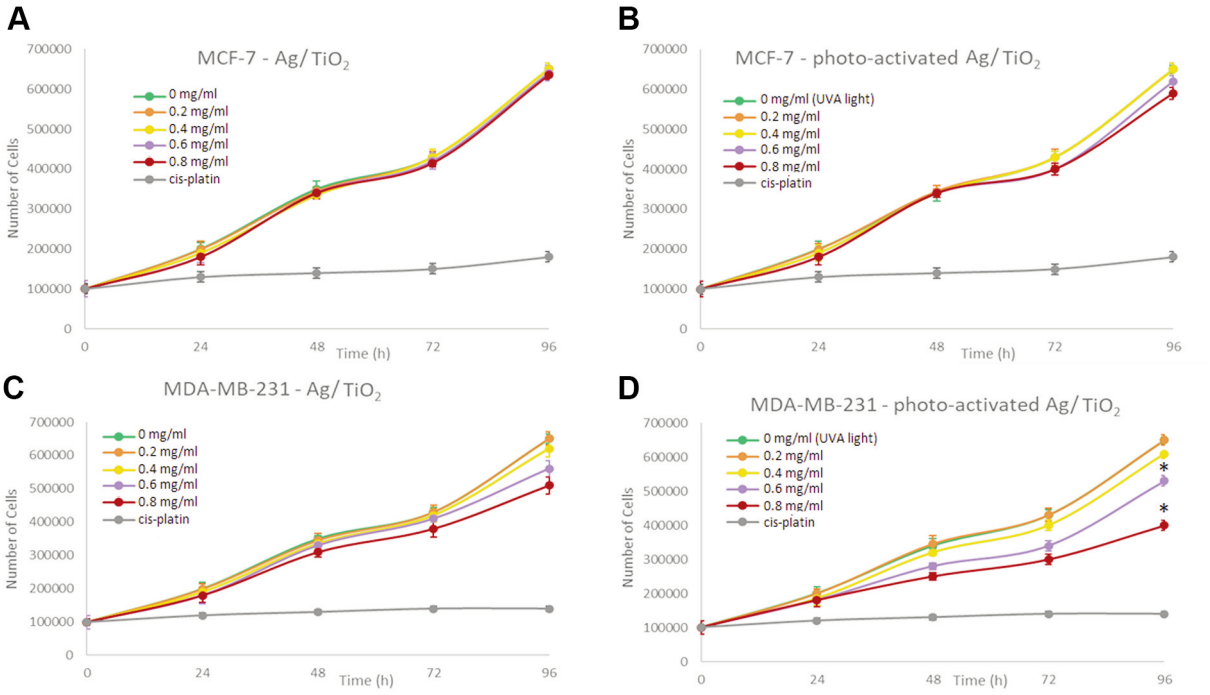

Figure 5. *Effect of Ag/TiO_2 NPs (silver-modified TiO_2 nanoparticles) on (A) MCF-7 (low metastatic potential) and (B) MDA-MB-231 (human breast adenocarcinoma, highly invasive) breast cancer epithelial cell proliferation. Effect of photoexcited Ag/TiO_2 NPs on the proliferation of (C) MCF-7 and (D) MDA-MB-231 breast cancer epithelial cells. Untreated cells were used as a negative control. Moreover, cells treated with UV-A light without TiO_2 were used as an extra negative control. As a positive control, cells treated for 24 h with cis-platin (0.8 mg/ml) were used. *$p<0.05$ vs. negative control (untreated) cells, based on the Kruskal-Wallis test. Data represent the mean±standard deviation from five independent experiments.*

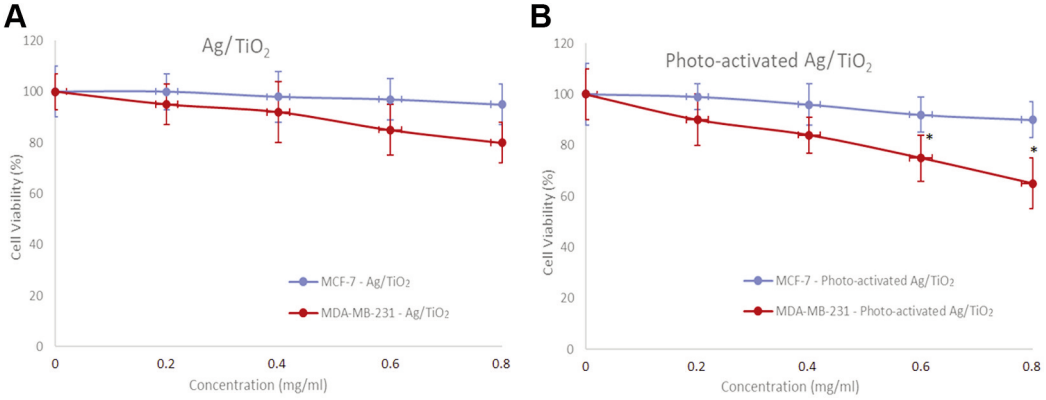

Figure 6. *Effect of (A) Ag/TiO_2 NPs (silver-modified TiO_2 nanoparticles) and (B) Photo-excited Ag/TiO_2 NPs on the viability of MCF-7 (low metastatic potential) and MDA-MB-231 (human breast adenocarcinoma, highly invasive) breast cancer epithelial cells. *$p<0.05$ vs. negative control, based on the Kruskal-Wallis test. MTT assay was employed to determine cell viability. Data represent means±standard deviation from five independent experiments.*

for 24 h with cisplatin (0.8 mg/ml) were used as a positive control for our experiment, inducing PARP cleavage.

Representative blots of uncleaved and cleaved PARP on both the cell lines are depicted in Figure 7. It is quite clear that PARP cleavage was remarkably increased in MDA-MB-231 cells treated with Ag/TiO_2 and, even more significantly, in those treated with photo-excited Ag/TiO_2 with UV-A, when comparing the obtained results with the untreated cells.

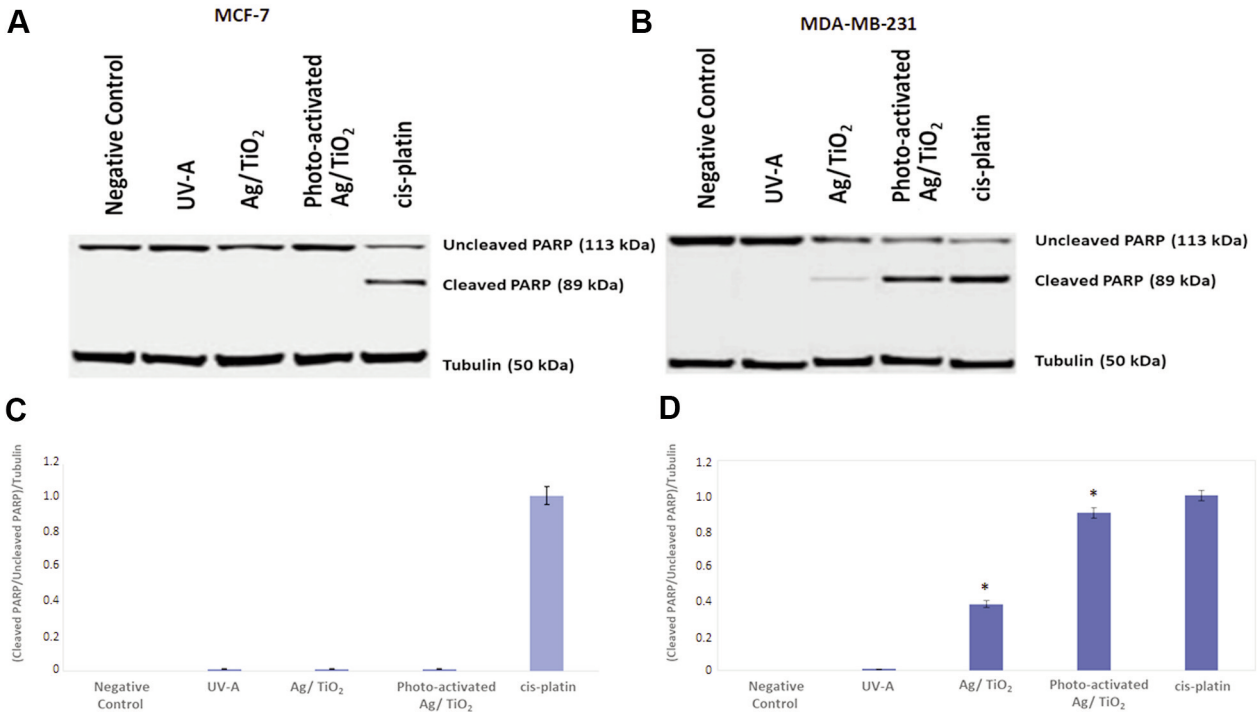

Figure 7. *Ag/TiO_2 NPs (silver-modified TiO_2 nanoparticles) and photo-activated Ag/TiO_2 NPs induce PARP cleavage. Representative immunoblots of cleaved and uncleaved PARP of MCF-7 (low metastatic potential) cells (A and C) and MDA-MB-231 (human breast adenocarcinoma, highly invasive) cells (B and D). Blots were probed with anti-tubulin antibody, to ensure equal protein levels in each sample. Quantification of cleaved/uncleaved PARP [poly(adenosine diphosphate ribose) polymerase] to tubulin levels for *p<0.05 was held, compared to the relevant ratio of untreated cells and based on the Kruskal-Wallis test. Cells treated with cisplatin (0.8 mg/ml) for 24 h were also used as a positive control for the induction of PARP cleavage. Data represent means±standard deviation from three independent experiments.*

These findings show that Ag/TiO_2 has the potential to induce apoptosis in MDA-MB-231 cells (Figure 7B and D). We did not detect PARP cleavage in MCF-7 cells, following the same procedure (Figure 7A and C).

The Bcl-2 family of proteins consists of a number of evolutionarily conserved members, playing crucial roles in cell apoptosis regulation, either promoting or inhibiting the cytochrome C release into the cytosol. This fact consequently triggers caspase-9 and caspase-3 activation and leads to apoptosis. More specifically Bcl-2 family proteins can regulate apoptosis by controlling mitochondrial outer membrane permeabilization (MOMP), a pivotal step in the apoptosis intrinsic pathway. Hence, the expression of the antiapoptotic factors Bcl-2 and Bcl-xL, as well as the expression of the proapoptotic factors Bax, and Bad was also examined to further clarify the apoptotic mechanism. Cells were treated with photoexcited Ag/TiO_2 and cell lysates were immunoblotted and probed with anti-Bcl-2, anti-Bcl-xL, anti-Bax, and anti-Bad antibodies. Cells treated for 24 h with cisplatin (0,8 mg/ml) were used as a positive control for apoptosis induction.

Representative immunoblots blots of Bax, Bcl-2, Bad and Bcl-xL expression, obtained from in both cell lines are presented in Figure 8. Ag/TiO_2 and more significantly photoexcited Ag/TiO_2 NPs led to an increase in Bax expression in MDA-MB-231 (Figure 9B and D), when compared to untreated cells. This finding is in agreement with the PARP cleavage that was found in the corresponding samples (Figure 7B and D). Moreover, a decrease in Bcl-2 expression was noticed in the same samples (Figure 9B and D). Under the same conditions, no significant effect was detected in MCF-7 cells in the expression of all the examined proteins (Bcl-2, Bax, Bcl-xL, Bad).

DNA-laddering assay. DNA-laddering assay is a widely used method for separation of DNA fragments, depending on their size and charge (38, 39). Cellular DNA damage treated with Ag/TiO_2 NPs was investigated through this assay. As shown in Figure 10, DNA fragmentation was induced by photo-excited Ag/TiO2 NPs and very slightly by Ag/TiO_2 NPs in MDA-MB-231 cells, if we compare these samples with the untreated cells (Figure 10B). The motif of fragmentation was quite similar to the fragmentation we noticed in the sample treated with cis-platin (0.8 mg/ml) for 24 h. Cells irradiated with UV-A exhibited no significant DNA fragmentation.

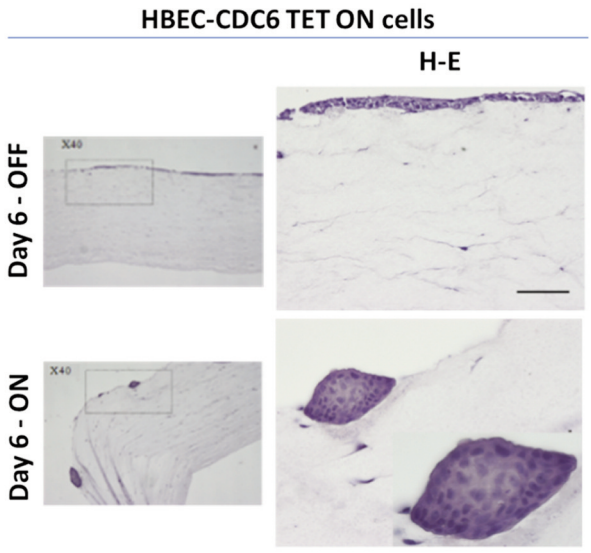

Figure 8. *Representative images of the HBEC (normal human bronchial epithelial cells) -CDC6 Tet ON cellular model, grown in 3D organotypic conditions and stained for H-E (hematoxylin-eosin). The epithelial origin of HBECs is similar to various other cancer types, and in their un-induced state [(A) "OFF" state], they lack mutations found in cancer cells. This 3D organotypic model allows the precise and reliable detection of amassing DNA alterations during CDC6-induced senescence [(B) "ON" state] (23).*

MCF-7 showed exactly what we have noticed in the previous experiments, *i.e.*, the DNA-laddering pattern was not detected (Figure 10A). These results are in accordance with the PARP cleavage (Figure 7) and Bax and Bcl-2 expression (Figure 9), indicating apoptosis.

Discussion

Nanostructured Ag/TiO_2 was synthesized *via* the sol-gel method. Enhanced photocatalytic activity was observed, since the time needed for the efficient photo-activation was approximately 10 min. Previous studies from our groups had shown that TiO_2 induced apoptosis only after a 20-min-irradiation with UV-A. Thus, silver modification allowed an optimization of the photocatalytic cytotoxicity that was controllably triggered in order to lead cancer cells to apoptosis. Full characterization, applying XRD, SEM, micro-Raman spectroscopy, UV-Vis spectroscopy and DLS verified the chemical modification TiO_2 with silver as well as the characteristics of the produced nanomaterial. The cytotoxicity tests (growth rates and MTT assay) of Ag/TiO_2 NPs have indicated inhibition in cell proliferation of the MDA-MB-231 cells. The MCF-7 cells were resistant to the treatment, thus no significant effect on cell proliferation was observed. The results of Ahamed *et al.* are in accordance with our findings as they also indicated that Ag/TiO_2 NPs did not cause cytotoxicity to human pulmonary cancer cells (A549) as well as MCF-7 cancer cells (40). They also found a cell-type selectivity, as they showed that Ag/TiO_2 NPs had a significant effect on cell viability of human liver cancer (HepG2) cells. Our results are in contrast with the results of Murugan *et al.* who reported that TiO_2 NPs exhibit a dose-dependent cytotoxicity in MCF-7 cells; however, the material they used is commercially available and non-modified. Moreover, the synthesis process is different and there was no photo-activation of the TiO_2 photocatalyst, thus any comparison of the results would not be based in the same experimental conditions (41).

Hence, we have shown that a selectivity of the produced Ag/TiO_2 toward specific cancer cells occurs. There were also various studies indicating that TiO_2 NPs can affect some of the cellular functions, such as inhibition of cell proliferation and decrease in viability when tested in human skin-derived cells (42). Many hypotheses have been proposed regarding the mechanism through which TiO_2 NPs potentially induce apoptosis or inhibit cell proliferation (32). TiO_2 particle-mediated cell toxicity could be interpreted, considering the interactions between cells and particles. However, to date, the specific interactions between TiO_2 NPs and membrane proteins are not totally understood. The surface characteristics of the TiO_2 NPs seem to be pivotal factors in the bioactivity the NPs (43). In addition, we have already completed a preliminary series of experiments, testing TiO_2 on Human Embryonic Kidney Cells (HEK293) and we have not detected any effect on cell viability. Among our aims is to investigate the biological effect of Ag/TiO_2 on various skin precancerous and melanoma cells, as we think that photo-activated Ag/TiO_2 might be used as a photosensitizer in an alternative photodynamic therapy, and thus superficial cancers like skin cancers would be the ideal biological system for this application.

The mechanism provoking this selectivity remains an unclarified field for further investigation. The possible mediated mechanism, that leads to the inhibition of cell proliferation is possibly through ROS generation, since previous studies also suggested that TiO_2 NPs create a large amount of reactive oxygen species, that may potentially lead to DNA damage (5, 44-46). Various studies indicate that TiO_2 NPs might induce apoptotic cell death in human non-small cell lung cancer cells (47), in human colon carcinoma cells (48) and others (32, 49, 50). This study aimed to evaluate the apoptotic potential of Ag/TiO_2 NPs. For this reason, two different breast cancer epithelial cell lines: the highly malignant MDA-MB-231 and the low metastatic MCF-7 cells. Our results showed that the efficacy of Ag/TiO_2 NPs to induce apoptosis in MDA-MB-231 cells was significant. Herein MDA-MB-231 cancer cells seemed to be more susceptible to apoptosis, induced by photo-excited Ag/TiO_2 NPs, compared to the lowly metastatic MCF-7 cells.

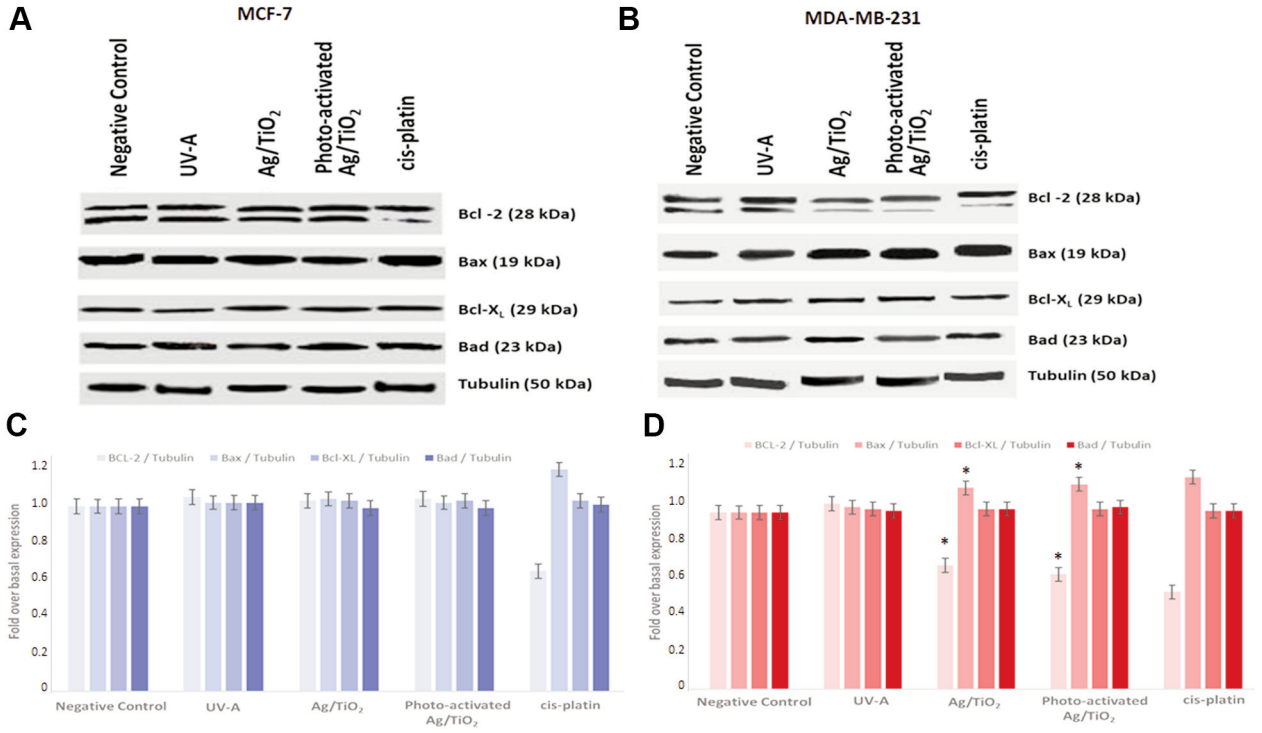

Figure 9. *Ag/TiO_2 NPs (silver-modified TiO_2 nanoparticles) and photo-activated Ag/TiO_2 NPs increased Bax expression and decreased Bcl-2 expression in MDA-MB-231 (human breast adenocarcinoma, highly invasive) cells. Representative immunoblots for Bcl-2, Bax, Bcl-xL and Bad expression in both cell lines are presented. Blots were also probed with anti-tubulin antibody for normalization. Densitometric quantification of Bcl-2/tubulin, Bax/tubulin, Bcl-xL/tubulin and Bad/tubulin as fold over basal rate (control cells) in (B and D) MDA-MB-231 cells and (A and C) MCF-7 (low metastatic potential) cells was performed, compared to the relevant ratios of untreated cells. Cells treated with cisplatin (0.8 mg/ml) for 24 h were also used as a positive control for the induction of Bcl-2 family of proteins deregulation. *$p<0.05$ vs. negative control, based on the Kruskal-Wallis test. Data represent means±standard deviation from three independent experiments.*

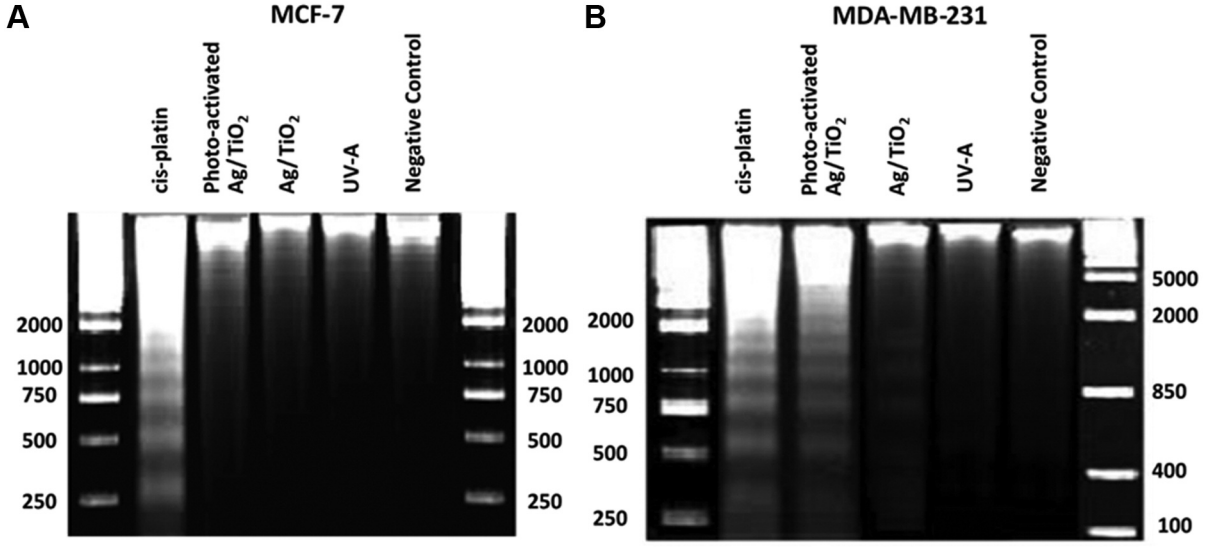

Figure 10. *Photo-activated Ag/TiO_2 NPs (silver-modified TiO_2 nanoparticles) induced DNA laddering in the MDA-MB-231 (human breast adenocarcinoma, highly invasive) cell line. Representative patterns of DNA laddering in (A) MCF-7 (low metastatic potential) and (B) MDA-MB-231 cells. Cells treated for 24 h with cisplatin (0.8 mg/ml) were used as positive controls for the induction of DNA laddering.*

Caspases play an important role in the apoptotic process, as their activation results in impaired cell function and programmed cell death (51). PARP is considered to be one of the main cleavage targets of caspases. During apoptosis, PARP is broken down into the inactive 89 and 24 kDa fragments. The DNA-binding domain of cleaved PARP is localized in the small fragment and it can thus inhibit access by other repair enzymes. The role of the big fragment (89 kDa) which is localized at the nucleoplasm during the apoptosis implementation, is to configure the activity of other proteins which are involved in apoptosis (*e.g.*, p53) (52).

Bcl-2 family proteins, regulating the mitochondrial permeability, also play an important role in cell apoptosis. Various studies demonstrated that TiO_2 NPs have the ability to induce apoptosis and are detected with increased expression of the proapoptotic protein Bax (53). We also indicated that photo-activated Ag/TiO_2 can increase the Bax expression and decrease the Bcl-2 levels in MDA-MB-231 cell line. Since it is known that during the late stages of apoptosis DNA fragmentation takes place (54), we also tried to certify the prevalent mechanism, through the DNA laddering assay. We noticed that DNA fragmentation took place in MDA-MB-231 cells.

Among our main perspectives is to focus our effort on the effect of the modified TiO_2 NPs on senescence, apart from apoptosis. We recently developed a cellular system based on normal human bronchial epithelial cells (HBECs) (23). HBEC system carries a CDC6-TetON overexpression cassette. The origin of HBECs is epithelia, like most common cancer types. Being at un-induced state ("OFF" state), HBECs are free from the mutation burden which is typically found in cancer cells. This permits precise and reliable detection of amassing DNA alterations during CDC6-induced senescence ("ON" state). It might be very promising to apply the modified TiO_2 NPs on the 3D-organotypic (Figure 8) cell culture conditions we have developed, which simulates a tissue related context, in addition to/as a substitute of *in vivo* studies.

Among our priorities is the optimization of the method by replacing ultraviolet with visible light. This is achievable through chemical modification with nitrogen, co-modification with metals and non-metals or even triple modification. The coating of the produced materials with smart polymers, stimuli responsive, such as the IP network microgel pNipam-co-PAA have shown promising results (5) and are still under investigation. The coating can modify the oxidative behavior of NPs and enhance their bioactivity. Green synthesis of silver is also in our plans. Based on some preliminary experiments we suggest these methods that are eco-friendly and avoid toxic reagents (55).

Our promising findings and others derived from our previous intensive studies (6, 7), demonstrate that photo-activated TiO_2 NPs can be considered as an anticancer agent that could be applied locally, followed by light irradiation focused on the tumor area. The cancer cells might be selectively affected by a light beam, introduced through a fiber optic close to a tumor region in parallel with a TiO_2 NPs injection. The great advantage of this potential therapeutic scheme is that TiO_2 NPs are biocompatible and thus they do not affect healthy tissues, avoiding the undesirable side effects of the traditional anticancer approaches.

Such an alternative approach based on the utilization of NPs might be very favourable, taking into account that the multidrug-resistance of the tumor cells remains a major obstacle to the success of chemotherapy.

Conclusion

Nanostructured Ag/modified TiO_2 was synthesized and characterized in order to be used for the investigation of their cytotoxicity on MCF-7 and MDA-MB-231 cells. An inhibition of cell proliferation on MDA-MB-231 cells was observed, while MCF-7 were unaffected. The precise molecular process involved in the preferential death of highly malignant cancer cells remains unclarified. Experiments for further investigation of this mechanism are in progress. However, our findings show that the TiO_2 nanoparticle cytotoxicity can upregulate the proapoptotic Bax expression, downregulating the antiapoptotic Bcl-2 expression. DNA damage and caspase-mediated PARP cleavage are also associated phenomena, and this means that cell apoptosis is the prevalent mechanism of cytotoxicity.

The design and development of an alternative photodynamic cancer therapy that can activated upon visible light irradiation, in parallel with a drug delivery approach, using smart polymers that might allow the controllable release of the catalyst in the biological system, maintaining the photo-induced activity of the smart composite. Our promising results show that photoexcited Ag/TiO_2 might be considered as an anticancer agent. Hence, an alternative approach based on the use of nanomaterials might be very intriguing, if we consider that multidrug-resistance of tumor cells is a common major obstacle to the success of a chemotherapy in addition to undesirable side effects.

Conflicts of Interest

The Authors declare that there are no conflicts of interest.

Authors' Contributions

Conceptualization V.G.G. and E.A.P.; investigation N.L., D.V., M.A.; supervision, V.G.G., E.A.P., M.G., P.F., E.-P. C. T., A.K.; funding acquisition, V.G.G.; methodology, N.L., A.K., I.P., A.B., T.F., D.S.T., P.K.; resources V.G.G., E.A.P., P.F., E.-P. C. T.; formal analysis N.L., A.P., K.E.; visualization N.L., D.V., K.E.; statistical analysis N.L., S.K.; validation N.L., A.K., K.E.; writing the original draft N.L., D.V., A.P., M.A., K.E.; writing, reviewing and editing N.L., P.F., I.P., T.F., E.-P.C.T., M.G., A.K., E.A.P. and V.G.G.

Funding

This study was financially supported by the National Public Investment Program of the Ministry of Development and Investment/General Secretariat for Research and Technology, in the framework of the of the Flagship Initiative to address SARS-CoV-2 (2020ΣΕ01300001). It was also supported by the Welfare Foundation for Social & Cultural Sciences, Athens, Greece (KIKPE); the Hellenic Foundation for Research and Innovation (HFRI) grants no. 775 and 3782 and NKUA-SARG grant 70/3/8916, by the kind donation of H. Pappas and by IKY scholarships program (action "Reinforcement of Postdoctoral Researchers", (N. Lagopati-scholarship for Postdoctoral Researchers-MIS5001552).

Acknowledgements

The Authors would like to acknowledge Labrini Sygellou for the XPS measurements performed in Surface Science Laboratory at the Foundation of Research and Technology Hellas, Institute of Chemical Engineering and High Temperature Chemical Processes (FORTH/ICE-HT) and Mrs. E. Kotsopoulou for her support.

References

1 Soares S, Sousa J, Pais A and Vitorino C: Nanomedicine: principles, properties, and regulatory issues. Front Chem 6: 360, 2018. PMID: 30177965. DOI: 10.3389/fchem.2018.00360

2 Seery M, George R, Floris P and Pillai S: Silver doped titanium dioxide nanomaterials for enhanced visible light photocatalysis. Journal of Photochemistry and Photobiology A: Chemistry *189(2-3)*: 258-263, 2019. DOI: 10.1016/j.jphotochem.2007.02.010

3 Lagopati N, Evangelou K, Falaras P, Tsilibary EC, Vasileiou PVS, Havaki S, Angelopoulou A, Pavlatou EA and Gorgoulis VG: Nanomedicine: Photo-activated nanostructured titanium dioxide, as a promising anticancer agent. Pharmacol Ther *222*: 107795, 2020. PMID: 33358928. DOI: 10.1016/j.pharmthera.2020.107795

4 Vamvakas I, Lagopati N, Andreou M, Sotiropoulos M, Gatzis A, Limouris G, Antypas C and Lyra M: Patient specific computer automated dosimetry calculations during therapy with 111In Octreotide. European Journal of Radiography *1(4)*: 180-183, 2018. DOI: 10.1016/j.ejradi.2010.08.001

5 Galata E, Georgakopoulou EA, Kassalia ME, Papadopoulou-Fermeli N and Pavlatou EA: Development of smart composites based on doped-TiO_2 nanoparticles with visible light anticancer properties. Materials (Basel) *12(16)*: 2589, 2019. PMID: 31416238. DOI: 10.3390/ma12162589

6 Lagopati N, Tsilibary EP, Falaras P, Papazafiri P, Pavlatou EA, Kotsopoulou E and Kitsiou P: Effect of nanostructured TiO_2 crystal phase on photoinduced apoptosis of breast cancer epithelial cells. Int J Nanomedicine *9*: 3219-3230, 2014. PMID: 25061298. DOI: 10.2147/IJN.S62972

7 Lagopati N, Kitsiou P, Kontos A, Venieratos P, Kotsopoulou E, Kontos A, Dionysiou D, Pispas S, Tsilibary E and Falaras P: Photo-induced treatment of breast epithelial cancer cells using nanostructured titanium dioxide solution. Journal of Photochemistry and Photobiology A: Chemistry *214(2-3)*: 215-223, 2019. DOI: 10.1016/j.jphotochem.2010.06.031

8 Kim H, Jeon D, Oh S, Nam K, Son S, Gye M and Shin I: Titanium dioxide nanoparticles induce apoptosis by interfering with EGFR signaling in human breast cancer cells. Environmental Research *175*: 117-123, 2019. PMID: 31112848. DOI: 10.1016/j.envres.2019.05.001

9 Gorgoulis V, Adams PD, Alimonti A, Bennett DC, Bischof O, Bishop C, Campisi J, Collado M, Evangelou K, Ferbeyre G, Gil J, Hara E, Krizhanovsky V, Jurk D, Maier AB, Narita M, Niedernhofer L, Passos JF, Robbins PD, Schmitt CA, Sedivy J, Vougas K, von Zglinicki T, Zhou D, Serrano M and Demaria M: Cellular senescence: defining a path forward. Cell *179(4)*: 813-827, 2019. PMID: 31675495. DOI: 10.1016/j.cell.2019.10.005

10 Muñoz-espín D: Nanocarriers targeting senescent cells. Translational Medicine of Aging *3*: 1-5, 2020. DOI: 10.1016/j.tma.2019.01.001

11 Liao C, Li Y and Tjong SC: Visible-light active titanium dioxide nanomaterials with bactericidal properties. Nanomaterials (Basel) *10(1)*: 124, 2020. PMID: 31936581. DOI: 10.3390/nano10010124

12 Barbouti A, Lagopati N, Veroutis D, Goulas V, Evangelou K, Kanavaros P, Gorgoulis VG and Galaris D: Implication of dietary iron-chelating bioactive compounds in molecular mechanisms of oxidative stress-induced cell ageing. Antioxidants (Basel) *10(3)*: 491, 2021. PMID: 33800975. DOI: 10.3390/antiox10030491

13 Fu YS, Li J and Li J: Metal/semiconductor nanocomposites for photocatalysis: fundamentals, structures, applications and properties. Nanomaterials (Basel) *9(3)*: 359, 2019. PMID: 30836647. DOI: 10.3390/nano9030359

14 Anaya-Esparza LM, Ruvalcaba-Gómez JM, Maytorena-Verdugo CI, González-Silva N, Romero-Toledo R, Aguilera-Aguirre S, Pérez-Larios A and Montalvo-González AE: Chitosan-TiO_2: A versatile hybrid composite. Materials (Basel) *13(4)*: 811, 2020. PMID: 32053948. DOI: 10.3390/ma13040811

15 Ilisz I and Dombi A: Investigation of the photodecomposition of phenol in near-UV-irradiated aqueous TiO2 suspensions. II. Effect of charge-trapping species on product distribution. Applied Catalysis A: General *180(1-2)*: 35-45, 2019. DOI: 10.1016/S0926-860X(98)00375-5

16 Etacheri V, Di valentin C, Schneider J, Bahnemann D and Pillai S: Visible-light activation of TiO2 photocatalysts: Advances in theory and experiments. Journal of Photochemistry and Photobiology C: Photochemistry Reviews *25*: 1-29, 2019. DOI: 10.1016/j.jphotochemrev.2015.08.003

17 Chao H, Yun Y, Xingfang H and Larbot A: Effect of silver doping on the phase transformation and grain growth of sol-gel titania powder. Journal of the European Ceramic Society *23(9)*: 1457-1464, 2020. DOI: 10.1016/S0955-2219(02)00356-4

18 Nbelayim P, Kawamura G, Kian Tan W, Muto H and Matsuda A: Systematic characterization of the effect of Ag@TiO_2 nanoparticles on the performance of plasmonic dye-sensitized solar cells. Sci Rep *7(1)*: 15690, 2017. PMID: 29146918. DOI: 10.1038/s41598-017-15541-z

19 Santos L, Machado W, França M, Borges K, Paniago R, Patrocinio A and Machado A: Structural characterization of Ag-doped TiO2 with enhanced photocatalytic activity. RSC Advances *5(125)*: 103752-103759, 2017. DOI: 10.1039/C5RA22647C

20 Piccinini F, Tesei A, Arienti C and Bevilacqua A: Cell counting and viability assessment of 2D and 3D cell cultures: Expected reliability of the trypan blue assay. Biological Procedures Online *19(1)*: 8, 2020. DOI: 10.1186/s12575-017-0056-3

21 Mosmann T: Rapid colorimetric assay for cellular growth and survival: application to proliferation and cytotoxicity assays. J Immunol Methods *65(1-2)*: 55-63, 1983. PMID: 6606682. DOI: 10.1016/0022-1759(83)90303-4

22 Plumb JA: Cell sensitivity assays: the MTT assay. Methods Mol Med *88*: 165-169, 2004. PMID: 14634227. DOI: 10.1385/1-59259-406-9:165

23 Komseli ES, Pateras IS, Krejsgaard T, Stawiski K, Rizou SV, Polyzos A, Roumelioti FM, Chiourea M, Mourkioti I, Paparouna E, Zampetidis CP, Gumeni S, Trougakos IP, Pefani DE, O'Neill E, Gagos S, Eliopoulos AG, Fendler W, Chowdhury D, Bartek J and Gorgoulis VG: A prototypical non-malignant epithelial model to study genome dynamics and concurrently monitor micro-RNAs and proteins in situ during oncogene-induced senescence. BMC Genomics *19(1)*: 37, 2018. PMID: 29321003. DOI: 10.1186/s12864-017-4375-1

24 Gelman A: Analysis of variance – why it is more important than ever. The Annals of Statistics *33(1)*: 1-53, 2021. DOI: 10.1214/009053604000001048

25 Acar E and Sun L: A generalized Kruskal–Wallis test incorporating group uncertainty with application to genetic association studies. Biometrics *69(2)*: 427-435, 2019. PMID: 23441822. DOI: 10.1111/biom.12006

26 Lee S and Lee DK: What is the proper way to apply the multiple comparison test? Korean J Anesthesiol *71(5)*: 353-360, 2018. PMID: 30157585. DOI: 10.4097/kja.d.18.00242

27 Patterson A: The Scherrer formula for X-ray particle size determination. Physical Review *56(10)*: 978-982, 2017. DOI: 10.1103/PhysRev.56.978

28 Li Z, Mi L, Wang PN and Chen JY: Study on the visible-light-induced photokilling effect of nitrogen-doped TiO2 nanoparticles on cancer cells. Nanoscale Res Lett *6(1)*: 356, 2011. PMID: 21711880. DOI: 10.1186/1556-276X-6-356

29 Stathatos E, Lianos P, Falaras P and Siokou A: Photocatalytically deposited silver nanoparticles on mesoporous TiO2Films. Langmuir *16(5)*: 2398-2400, 2019. DOI: 10.1021/la981783t

30 López R and Gómez R: Band-gap energy estimation from diffuse reflectance measurements on sol–gel and commercial TiO2: a comparative study. Journal of Sol-Gel Science and Technology *61(1)*: 1-7, 2019. DOI: 10.1007/s10971-011-2582-9

31 Sanchez-martinez A, Ceballos-sanchez O, Koop-santa C, López-mena E, Orozco-guareño E and García-guaderrama M: N-doped TiO2 nanoparticles obtained by a facile coprecipitation method at low temperature. Ceramics International *44(5)*: 5273-5283, 2020. DOI: 10.1016/j.ceramint.2017.12.140

32 Thevenot P, Cho J, Wavhal D, Timmons RB and Tang L: Surface chemistry influences cancer killing effect of TiO2 nanoparticles. Nanomedicine *4(3)*: 226-236, 2008. PMID: 18502186. DOI: 10.1016/j.nano.2008.04.001

33 Hero T, Bühler H, Kouam PN, Priesch-Grzeszowiak B, Lateit T and Adamietz IA: The triple-negative breast cancer cell line MDA-MB 231 is specifically inhibited by the ionophore salinomycin. Anticancer Res *39(6)*: 2821-2827, 2019. PMID: 31177119. DOI: 10.21873/anticanres.13410

34 Croker AK, Goodale D, Chu J, Postenka C, Hedley BD, Hess DA and Allan AL: High aldehyde dehydrogenase and expression of cancer stem cell markers selects for breast cancer cells with enhanced malignant and metastatic ability. J Cell Mol Med *13(8B)*: 2236-2252, 2009. PMID: 18681906. DOI: 10.1111/j.1582-4934.2008.00455.x

35 Satoh MS and Lindahl T: Role of poly(ADP-ribose) formation in DNA repair. Nature *356(6367)*: 356-358, 1992. PMID: 1549180. DOI: 10.1038/356356a0

36 Alvarez-Gonzalez R, Spring H, Müller M and Bürkle A: Selective loss of poly(ADP-ribose) and the 85-kDa fragment of poly(ADP-ribose) polymerase in nucleoli during alkylation-induced apoptosis of HeLa cells. J Biol Chem *274(45)*: 32122-32126, 1999. PMID: 10542247. DOI: 10.1074/jbc.274.45.32122

37 Oliver FJ, de la Rubia G, Rolli V, Ruiz-Ruiz MC, de Murcia G and Murcia JM: Importance of poly(ADP-ribose) polymerase and its cleavage in apoptosis. Lesson from an uncleavable mutant. J Biol Chem *273(50)*: 33533-33539, 1998. PMID: 9837934. DOI: 10.1074/jbc.273.50.33533

38 Satkauskas S, Bureau MF, Puc M, Mahfoudi A, Scherman D, Miklavcic D and Mir LM: Mechanisms of *in vivo* DNA electrotransfer: respective contributions of cell electropermeabilization and DNA electrophoresis. Mol Ther *5(2)*: 133-140, 2002. PMID: 11829520. DOI: 10.1006/mthe.2002.0526

39 Brody JR and Kern SE: History and principles of conductive media for standard DNA electrophoresis. Anal Biochem *333(1)*: 1-13, 2004. PMID: 15351274. DOI: 10.1016/j.ab.2004.05.054

40 Ahamed M, Khan MAM, Akhtar MJ, Alhadlaq HA and Alshamsan A: Ag-doping regulates the cytotoxicity of TiO_2 nanoparticles *via* oxidative stress in human cancer cells. Sci Rep *7(1)*: 17662, 2017. PMID: 29247182. DOI: 10.1038/s41598-017-17559-9

41 Murugan K, Dinesh D, Kavithaa K, Paulpandi M, Ponraj T, Alsalhi MS, Devanesan S, Subramaniam J, Rajaganesh R, Wei H, Kumar S, Nicoletti M and Benelli G: Hydrothermal synthesis of titanium dioxide nanoparticles: mosquitocidal potential and anticancer activity on human breast cancer cells (MCF-7). Parasitol Res *115(3)*: 1085-1096, 2016. PMID: 26621285. DOI: 10.1007/s00436-015-4838-8

42 Kiss B, Bíró T, Czifra G, Tóth BI, Kertész Z, Szikszai Z, Kiss AZ, Juhász I, Zouboulis CC and Hunyadi J: Investigation of micronized titanium dioxide penetration in human skin xenografts and its effect on cellular functions of human skin-derived cells. Exp Dermatol *17(8)*: 659-667, 2008. PMID: 18312389. DOI: 10.1111/j.1600-0625.2007.00683.x

43 Huerta-García E, Zepeda-Quiroz I, Sánchez-Barrera H, Colín-Val Z, Alfaro-Moreno E, Ramos-Godinez MDP and López-Marure R: Internalization of titanium dioxide nanoparticles is cytotoxic for H9c2 rat cardiomyoblasts. Molecules *23(8)*: 1955, 2018. PMID: 30082584. DOI: 10.3390/molecules23081955

44 Abdal Dayem A, Hossain MK, Lee SB, Kim K, Saha SK, Yang GM, Choi HY and Cho SG: The role of reactive oxygen species (ROS) in the biological activities of metallic nanoparticles. Int J Mol Sci *18(1)*: 120, 2017. PMID: 28075405. DOI: 10.3390/ijms18010120

45 Yu Z, Li Q, Wang J, Yu Y, Wang Y, Zhou Q and Li P: Reactive oxygen species-related nanoparticle toxicity in the biomedical field. Nanoscale Res Lett *15(1)*: 115, 2020. PMID: 32436107. DOI: 10.1186/s11671-020-03344-7

46 Chibber S: Titanium dioxide (Tio2) nanoparticles induced ROS generation and its effect on cellular antioxidant defense in WRL-68 cell. MOJ Bioequivalence & Bioavailability *3(3)*: 70-74, 2019. DOI: 10.15406/mojbb.2017.03.00036

47 Wang Y, Cui H, Zhou J, Li F, Wang J, Chen M and Liu Q: Cytotoxicity, DNA damage, and apoptosis induced by titanium dioxide nanoparticles in human non-small cell lung cancer A549 cells. Environ Sci Pollut Res Int *22(7)*: 5519-5530, 2015. PMID: 25339530. DOI: 10.1007/s11356-014-3717-7

48 De Angelis I, Barone F, Zijno A, Bizzarri L, Russo MT, Pozzi R, Franchini F, Giudetti G, Uboldi C, Ponti J, Rossi F and De Berardis B: Comparative study of ZnO and TiO□ nanoparticles: physicochemical characterisation and toxicological effects on human colon carcinoma cells. Nanotoxicology *7(8)*: 1361-1372, 2013. PMID: 23078188. DOI: 10.3109/17435390.2012.741724

49 Warheit DB, Webb TR, Reed KL, Frerichs S and Sayes CM: Pulmonary toxicity study in rats with three forms of ultrafine-TiO2 particles: differential responses related to surface properties. Toxicology *230(1)*: 90-104, 2007. PMID: 17196727. DOI: 10.1016/j.tox.2006.11.002

50 Behnam MA, Emami F, Sobhani Z and Dehghanian AR: The application of titanium dioxide (TiO_2) nanoparticles in the photo-thermal therapy of melanoma cancer model. Iran J Basic Med Sci *21(11)*: 1133-1139, 2018. PMID: 30483386. DOI: 10.22038/IJBMS.2018.30284.7304

51 Elmore S: Apoptosis: a review of programmed cell death. Toxicol Pathol *35(4)*: 495-516, 2007. PMID: 17562483. DOI: 10.1080/01926230701320337

52 Chaitanya GV, Steven AJ and Babu PP: PARP-1 cleavage fragments: signatures of cell-death proteases in neurodegeneration. Cell Commun Signal *8*: 31, 2010. PMID: 21176168. DOI: 10.1186/1478-811X-8-31

53 Gross A and Katz SG: Non-apoptotic functions of BCL-2 family proteins. Cell Death Differ *24(8)*: 1348-1358, 2017. PMID: 28234359. DOI: 10.1038/cdd.2017.22

54 Lagopati N, Belogiannis K, Angelopoulou A, Papaspyropoulos A and Gorgoulis V: Non-canonical functions of the ARF tumor suppressor in development and tumorigenesis. Biomolecules *11(1)*: 86, 2021. PMID: 33445626. DOI: 10.3390/biom11010086

55 Lagopati N, Gatou MA, Tsoukleris DS and Pavlatou EA: Biogenic synthesis of silver nanoparticles with antimicrobial properties. Nanomed Nanotechnol *5(2)*: 000185, 2020. DOI: 10.23880/nnoa-16000185

Received April 12, 2021
Revised April 24, 2021
Accepted April 26, 2021